# Variations of Aerosol and Wet Deposition in Hong Kong: Preliminary Results

Long S. CHIU, Kwok-cheung LOK

Institute of Space and Earth Information Science Chinese University of Hong Kong, Shatin NT Hong Kong SAR, PRC
E-mail: longchiu@cuhk.edu.hk

**Abstract**

Examination of Air Pollution Index (API) for the period 2000-2007 in Hong Kong general monitoring stations showed a summer maximum in Kwai Chung and winter maximum in Yuen Long. There is an east-west asymmetry, with higher API in the western than the eastern part of Hong Kong, which is consistent with Aerosol Optical Depth(AOD) pattern derived from the NASA/Moderate Resolution Imaging Spectroradiometer (MODIS). Cross boarder transport of pollution in Hong Kong was examined by compiling API data according to daily prevailing wind directions. In winter, the API is significantly higher when the prevailing wind direction is northerly and significantly lower for southerly flows. Assuming the API during southerly flow is the in situ ambient API, the cross border transports are estimated to be 33% and 23%, respectively for summer and winter. Both the AOD and API showed increase from 2000 to 2004, followed by slight dip and increases again to a secondary maximum in 2007. The decline may be related to the adoption of environmental policies and laws in Hong Kong and in Pearl River Delta region for the period. The scavenging of aerosol by rain is examined using changes in daily API after rain days. Our result showed a significant negative correlation between percentage decrease in API and rain rate for the winter, however, no significant empirical relation exists for the summer. This may be related to dynamics of rain clouds which overwhelms the microphysical effects in summer and points to the use of finer scale, such as hourly data to quantify the scavenging effect.

**Keywords**

cross border pollution transport, MODIS, API, AOD, Hong Kong-Guangzhou

## I. INTRODUCTION

Aerosols are suspended particulates in air. Around 90% of the atmospheric aerosol is produced by or as a result of human activities such as burning of fossil fuel, vehicular exhaust, while the remaining 10% is produced by natural sources such as volcanic eruption, sea spray (Wallace and Hobb, 1977). They affect the visibility, atmospheric radiation balance, cloud nucleation and hence the rain formation processes (Lohmann, 2006). The relation between aerosol and atmospheric visibility and the radiative budget has been examined by many. For example, Yuet and Sequeira (2000) and Leaderer et al. (1979) showed an inverse relationship of water soluble aerosol and visibility degradation in Hong Kong. Dickinson (1996) found that increases in the amount of aerosol can increase the cloud amount, increasing the heat trapped from the sun and altered the global energy balance.

Aerosol interaction with drops and precipitation is a traditional problem in cloud physics (Sinkevich, 2003). Lohmann (2006) used ECHAM5 general circulation model to estimate aerosol effects on convective clouds. She found that in the area with high aerosol concentration, the drizzle formation is reduced because of cloud droplet number increased. Faster aerosol removal also results in smaller increase in liquid water path when going from pre-industrial times to present. Lohmann and Feichter (2005) investigated the effects aerosols produced from fire smoke to precipitation. They found that smoke from sugarcane and forest fires reduced cloud droplet size and inhibit precipitation. Rosenfeld (1999) and Rosenfeld and Woodley (2000) argued that pollution aerosols suppress deep convective precipitation by decreasing cloud droplet size and delaying the onset of freezing. Khain et al. (2005) suggested that smaller cloud droplets, such as those originated from human activities would reduce drizzle rain. Precipitation from single mixed phase clouds is reduced under continental and marine time conditions when aerosol concentration increased. From the above literatures, we can conclude that aerosol generally suppresses precipitation formation especially on drizzle rain.

Wet deposition by cloud and precipitating particles is a major removal mechanism of aerosol particles. Atmospheric aerosol may be scavenged by precipitation due to Brownian diffusion, thermo and diffusiophoretic forces, inertial impaction, electrical forces and by serving as cloud condensation nuclei. Chate et al. (2003) suggested that below cloud scavenging mainly affects the particles in coarse mode and fine particles mode remains unchanged for all suspended particulates. The same result was also found by Garcia et al. (1994). However, there is still no clear evidence of particle size dependence for scavenging over remote marine regions (Baut-Menard Pand Duce, R.A, 1996). Chate et al. also suggested that different chemical properties, particularly the solubility of particles of different sizes may also play a role on the scavenging efficiency. Furthermore, Sinkevich (2003) suggested that the effect of scavenging was the most distinct in long time intensive precipitation on aerosol. The effect of scavenging takes place during 1–2 hours after precipitation. However, the effect of significant but short duration precipitation does not follow

1082-4006/08/14(02)-92$5.00

that of long duration precipitation. The aerosol was scavenged only within 30 minutes. Therefore, the above researches suggested that precipitation will more efficiently scavenge the coarse mode aerosol, compared with the fine mode one. Chemical properties of aerosol and the magnitude of rain also alter the efficiency of scavenging.

Because of its geographical location, the air pollution in Hong Kong is affected both by local generation and transport from the surrounding areas, such as the Pearl River Delta (PRD) region. This region has seen tremendous economic and population growth in recent years and pollution goes with it. Power plant generation, vehicular and ship exhaust are the major emission sources. The major types of pollutants are sulphur dioxide, nitrous oxide, Respirable suspended particulates (RSP), volatile organic compound (VOC) and carbon monoxide. (EPD, 2008) Most of the sulfur dioxide is generated by electricity generation while the transportation sector contributes mostly to nitrous oxide, carbon monoxide and RSP (HKEPD, 2008). The HKEPD adopted an air pollution index (API) that merges the pollutants. The elimination of sulfur bearing fuels reduces the API substantially since 1990.

The HK Environmental Protection Department (HKEPD) report on air quality in the Pearl River Delta Region (HKEPD, 2003) found that certain air pollutants can impact locations far from their sources and contribute to air pollution over geographically large areas like the PRD Region. The study showed that the most dominant types of cross boarder pollutants are ozone, RSP and nitrogen dioxide. Ozone content is the highest in spring and autumn while nitrogen dioxide and RSP concentration is high in winter and it was confirmed that considerable amount of the above pollutants comes from regional pollutants. Lau et al. (2007) conducted a survey to investigate the impact of cross border pollution to Hong Kong. They showed that regional influence on Hong Kong's air quality contributed to 132 heavy polluted days in a year (approximately 36% of the time) while local sources are the crucial factor for 53% of the time (on 192 days), while the remaining 11% are low pollution days (Lau, et al., 2007).

The objectives of this work are to:

- Examine the spatial and temporal distribution of aerosol concentration in Hong Kong.
- Quantify the impact of cross border transport of HK aerosol distribution
- Examine the utility of satellite derived products in complementing in situ data for monitoring regional pollution
- Investigate the efficiency of wet deposition of aerosol by precipitation

The spatial and temporal distribution of air pollution in Hong Kong is first examined using an Air Pollution Index (API) and a satellite derived Aerosol Optical Thickness (AOT). Cross border transport is examined by compiling API statistics according to the prevailing wind direction. The trends observed are examined in terms of the environmental policies adopted for the region. Section II describes the data and methodology. Section III discusses the analysis and results. Section IV concludes our work and discusses further study plans.

## II. DATA

The aerosol optical depth (AOD) data are retrieved from measurements taken by the MODerate resolution Imaging SpectroRadiometer (MODIS) on board NASAs' Eos (Terra and Aqua) satellites. Terra orbit passes from north to south across the equator in the morning while Aqua passes north to south over the equator in the afternoon. Terra MODIS and Aqua MODIS are viewing the entire Earth's surface every 1 to 2 days, acquiring data in 36 spectral bands in the visible and infrared. AOD is estimated from information derived from the 0.55μm band.

Daily meteorological data, including wind direction and rainfall amount are available from the Hong Kong Observatory web site. The wind direction and rainfall data at King's Park are used. The HKEDP monitored pollution at eleven general and three roadside stations. Hourly API data are tabulated in Excel Spreadsheets and can be easily downloaded. API is the conversion of the ambient respirable suspended particulate (RSP), sulfur dioxide ($SO_2$), carbon monoxide (CO), ozone ($O_3$) and nitrogen dioxide ($NO_2$) concentrations. While AOD is a columnar integrated amount, the API provides information at the surface. Aerosols are transported by the atmosphere and can be confined in thin atmospheric layers and there may not be a one-to-one correspondence between AOD and API. However, recent researches suggest that remote sensing technique can provide AOD information at higher resolution (Wong, et al., 2008, this issue) and for surface (He, et al., 2008).

Figure 1 shows the distribution of general and roadside pollution monitoring stations in Hong Kong.

A Students' t-test for sample versus population is used to test if API for different wind directions are different (Bulmer, 1979). Let $m$ be the sample mean for size $n$ and $\mu$ and $\sigma$ are the mean and standard deviation of population. The null hypothesis that there is no difference between the sample and the population will be rejected if the t score exceeds ~2 for the 95% level of significance

$$t' = (m-\mu)/\sqrt{(\sigma^2/n)}$$

To detect linear trends, we use regression analysis of the form

$$X(t) = at + b$$

Where $a$ is the slope and $b$ the intercept of the regression and $t$ is time. The null hypothesis that $a = 0$ is tested. If $a$ deviates significantly from zero, we say that there is a linear trend (increasing if $a$ >0 and decreasing if $a$ <0). The significance of


**Figure 1.** Distribution of general and roadside monitoring stations in Hong Kong.(Courtesy HKEPD URL http://www.epd-asg.gov.hk/english/backgd/quality.php)

$a$ is tested using the p-value which are available from statistical packages such as SPSS. SPSS Ver. 15.0 and Microsoft Excel are used for all statistical analysis and graphics.

## III. ANALYSIS AND RESULTS

Table 1 shows the average API for the general stations for winter months (November–February) and summer months (June–September).

To examine the spatial distribution, the station with the maximum API in each year is colored orange. Yuen Long consistently shows the largest API value in winter. If we consider the median of the station API observations, there is in general an asymmetry of API observations, with higher API in the stations in the western part of HK than those in the eastern part. For example, for the winter average, the median is Kwai Chung with an API of 53.9. Station in Yuen Long,

**Table 1.** Seasonal and annual average API for station in Central/Western (C/W), Eastern (E), Kwai Chung (KC), Kwun Tong (KT), Shatin (ST), Shum Shui Po (SSP), Tai Po (TP), Tap Mun (TM), Tsuen Wan (TW), Tung Chung (TC) and Yuen Long (YL) for winter (a), summer (b) and their average (c). The station with the (spatial) maximum for each year is colored orange and the year of (temporal) maximum API for each station is colored blue. Missing data are coded "–"

(a) Winter

| Winter | C/W | E | KC | KT | ST | SSP | TP | TM | TW | TC | YL |
|---|---|---|---|---|---|---|---|---|---|---|---|
| 2000 | 50.01 | 45.84 | 51.21 | 51.74 | 45.45 | 50.69 | 46.59 | 40.38 | 51.53 | 49.81 | 53.87 |
| 2001 | 53.39 | 47.85 | 51.75 | 56.84 | 47.87 | 53.52 | 48.53 | 44.07 | 51.02 | 50.64 | 56.71 |
| 2002 | 47.02 | 47.68 | 52.02 | 56.83 | 47.24 | 54.36 | 48.49 | 41.61 | 52.60 | 51.32 | 55.17 |
| 2003 | 57.82 | 53.59 | 59.72 | 60.97 | 54.83 | 58.53 | 56.10 | 50.98 | 61.09 | 59.02 | 62.07 |
| 2004 | 56.29 | 53.85 | 58.52 | 56.53 | 54.55 | 57.44 | 51.51 | 52.37 | 58.28 | 58.90 | 61.82 |
| 2005 | 54.65 | 50.17 | 54.25 | 52.58 | 52.45 | 54.88 | 49.81 | 50.75 | 56.28 | 58.94 | 61.84 |
| 2006 | 54.26 | 49.83 | 53.78 | 53.08 | 52.47 | 56.68 | 53.42 | 48.82 | 55.33 | 56.35 | 58.93 |
| 2007 | 55.96 | 53.44 | 58.20 | 54.84 | 55.26 | 59.47 | 55.28 | 54.68 | 58.33 | 59.08 | 63.17 |
| average | 53.67 | 50.28 | 54.93 | 55.42 | 51.27 | 55.70 | 51.22 | 47.96 | 55.55 | 55.51 | 59.20 |

(b) Summer

| Summer | C/W | E | KC | KT | ST | SSP | TP | TM | TW | TC | YL |
|---|---|---|---|---|---|---|---|---|---|---|---|
| 2000 | 31.70 | 29.14 | 42.39 | 37.38 | 31.91 | 36.67 | 33.96 | 27.39 | 35.12 | 27.96 | 36.52 |
| 2001 | 35.80 | 30.61 | 41.54 | 39.75 | 34.36 | 41.23 | 34.71 | 28.17 | 37.31 | 30.45 | 36.05 |
| 2002 | 30.15 | 29.40 | 39.39 | – | 33.48 | 36.59 | 32.45 | 28.55 | 38.43 | 30.06 | 35.16 |
| 2003 | 29.48 | 29.85 | 40.51 | 34.93 | 27.53 | 34.55 | 32.86 | 27.27 | 37.96 | 28.74 | 33.93 |
| 2004 | 38.85 | 37.24 | 44.16 | 41.47 | 38.89 | 42.78 | – | 32.66 | 42.98 | 38.97 | 44.33 |
| 2005 | 33.52 | 31.85 | 40.34 | 38.02 | 32.56 | 35.17 | 32.03 | 32.24 | 36.07 | 31.00 | 34.35 |
| 2006 | 33.20 | 30.52 | 39.43 | 36.37 | 35.62 | 36.67 | 35.61 | 33.89 | 37.83 | 32.65 | 36.14 |
| 2007 | 28.93 | 29.26 | 40.75 | 35.43 | 31.40 | 34.85 | 30.61 | 28.84 | 36.11 | 27.15 | 34.20 |
| average | 32.70 | 30.98 | 41.06 | 37.62 | 33.22 | 37.31 | 33.18 | 29.88 | 37.73 | 30.87 | 36.33 |

(c) Average

| Annual | C/W | E | KC | KT | ST | SSP | TP | TM | TW | TC | YL |
|---|---|---|---|---|---|---|---|---|---|---|---|
| 2000 | 40.86 | 37.49 | 46.80 | 44.56 | 38.68 | 43.68 | 40.27 | 33.89 | 43.33 | 38.88 | 45.19 |
| 2001 | 44.59 | 39.23 | 46.65 | 48.29 | 41.11 | 47.37 | 41.62 | 36.12 | 44.17 | 40.55 | 46.38 |
| 2002 | 38.58 | 38.54 | 45.70 | – | 40.36 | 45.47 | 40.47 | 35.08 | 45.52 | 40.69 | 45.17 |
| 2003 | 43.65 | 41.72 | 50.11 | 47.95 | 41.18 | 46.54 | 44.48 | 39.12 | 49.52 | 43.88 | 48.00 |
| 2004 | 47.57 | 45.55 | 51.34 | 49.00 | 46.72 | 50.11 | – | 42.52 | 50.63 | 48.93 | 53.08 |
| 2005 | 44.08 | 41.01 | 47.29 | 45.30 | 42.51 | 45.03 | 40.92 | 41.49 | 46.17 | 44.97 | 48.10 |
| 2006 | 43.73 | 40.18 | 46.60 | 44.72 | 44.05 | 46.68 | 44.51 | 41.35 | 46.58 | 44.50 | 47.53 |
| 2007 | 42.44 | 41.35 | 49.47 | 45.14 | 43.33 | 47.16 | 42.95 | 41.76 | 47.22 | 43.11 | 48.68 |
| average | 43.19 | 40.63 | 48.00 | 46.42 | 42.24 | 46.50 | 42.18 | 38.92 | 46.64 | 43.19 | 47.77 |

Tsuen Wan, Tung Chung, Sham Shui Po and Kwun Tong show higher APIs whereas other stations have lower APIs. Tap Mum shows the lowest API, however, it shows an increase in recent years, with station Eastern basically sharing the minimum in the 2007 winter. Kwai Chung shows the maximum API in summer, except for 2004 when it is a close second to Yuen Long. A similar west-east asymmetric pattern can be found for the summer.

Figure 2 shows the histogram of station seasonal AIP for winter and summer. There is a distinct separation between the seasons; the API in winter is significantly higher (at 95% level) than that in summer.

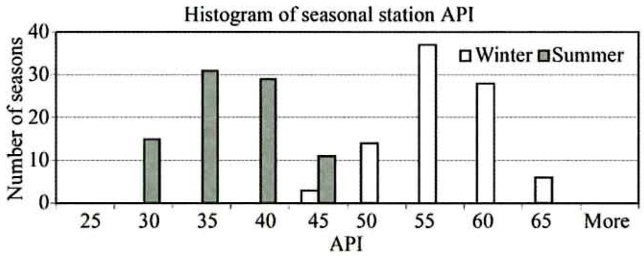


**Figure 2.** Histogram of station seasonal API for summer and winter

The long-term average AOD at 0.55μm derived from MODIS is shows in Figure 3. There is a maximum AOD centering in the west side of the Pearl River Delta, with AOD values in excess of 0.9. The general pattern of AOD in Hong Kong shows a general west-east asymmetry, which is consistent with API distribution.

How is Hong Kong affected by the high AOD in the Pearl River Delta region? We compile API values according to the daily wind direction observed at the HKO. The directions are classified as North (N, 316°–45°), East(E, 46°–135°), South (S, 136°–225°) and West (W, 226°–315°).

Table 2 shows the means and standard deviations of API for the four wind directions. Bordered by the ocean to the south, southerly flow represents the absence of transport from the PRD. Student's t-tests (Bulmer, 1979) for samples of API for each wind directions against the population are performed and the results are shown in the last column. T-statistics higher than two are significant at the 95% level. The lowest API is recorded for southerly (wind from the south) for both seasons while highest API is recorded when the wind is northerly in summer and westerly in winter. It should be noted that the APIs are higher with westerly flow for both seasons. The t-statistics show that in winter, there is no distinct difference of API for the four wind directions. The winter wind direction distribution is skewed, with winds from the north and east contributing to most of the daily observations. On the other hand, the wind direction distribution is fairly even in summer; the t-statistics show that the API is significantly higher for northerly($t$ = 8.96) and significantly lower for southerly ($t$=–6.52) wind.

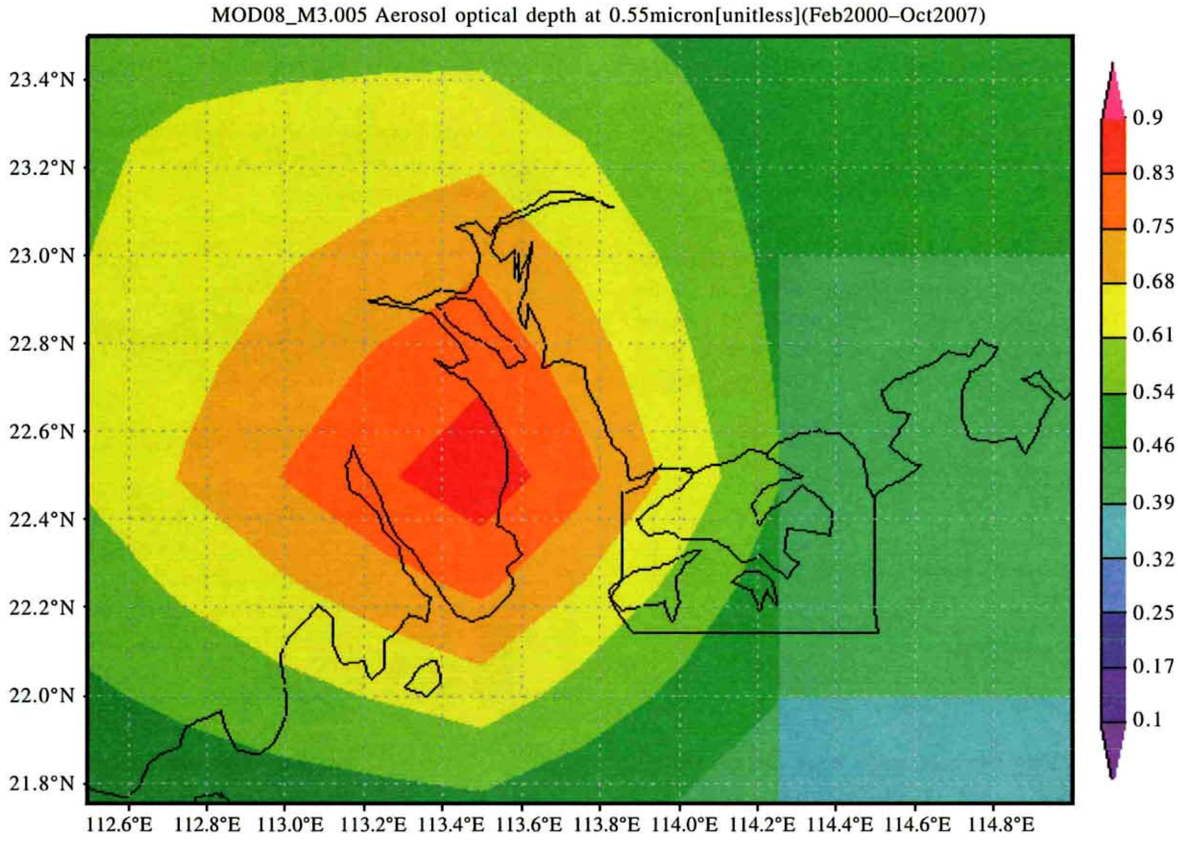


**Figure 3.** Distribution of MODIS 0.55μm AOD over the Pearl River Delta Region

**Table 2.** Mean and standard deviation (SD) of daily API in winter and summer and for different wind direction from 2000–2007. The last column shows the Student t-test of the difference between the ensemble means for each wind direction category and the population mean. T-scores larger than 2 are significant at the 95% level

| Wind direction | N | Mean | Std. Deviation | $t$-stat |
|---|---|---|---|---|
| Winter total | 902 | 58.31 | 14.97 | |
| north | 416 | 56.98 | 13.76 | −1.82 |
| east | 473 | 59.536 | 12.10 | 1.75 |
| south | 9 | 50.83 | 11.64 | −1.50 |
| west | 4 | 71.47 | 7.03 | 1.76 |
| Summer total | 980 | 39.26 | 15.07 | |
| north | 108 | 52.20 | 14.98 | 8.96 |
| east | 384 | 38.54 | 13.33 | −0.94 |
| south | 225 | 32.74 | 10.36 | −6.52 |
| west | 263 | 40.58 | 16.03 | 1.43 |

To examine the long-term trends, the year of maximum API is colored blue in Table 1. The API showed a maximum in 2004 in most stations for both seasons, except for Tap Mum, Sham Shui Po, Tung Chung and Yuen Long, which showed maxima in the 2007 winter.

Figure 4 shows the time series of the annual average for general monitoring stations in the west (Yuen Long, Tsuen Wan, Kwai Chung, Tung Chung, Sham Shui Po, and Central/Western, denoted HK West) and in the east (Tai Po, Shatin, Tap Mun, Kwun Tong, and Eastern, denoted HK East) and the average of all stations. The summer and winter averages are included for comparison. The missing data are filled with climatology. The HK West, HK East and annual all showed maxima in 2004. The decline actually started in summer 2003, as the time series of summer API is a maximum in 2003. Linear trend analysis for the whole period (2000–2007) showed an insignificant (p-value >0.05) trend of 0.48/year. Analysis using only data for the early period (2000–2004) indicates a linear trend of 1.52/year, with a p-value of 0.03, which is significant at the 95% level. This break in the increasing trend is also noted in the HKEPD reports.

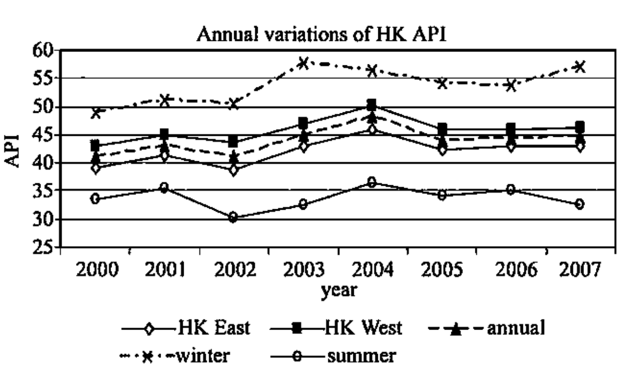


**Figure 4.** Yearly variations of API for annual average of HK East, HK West, annual mean, and the average for winter and summer

Atmospheric pollution affects the visibility. The hours of reduced visibility (< 8km) are recorded at the HKO and at the airport, situated to the north west of Tung Chung. Figure 5 shows the time series of total hours of poor visibility at these stations. The number of poor visibility in the Airport is higher than that at the HKO.

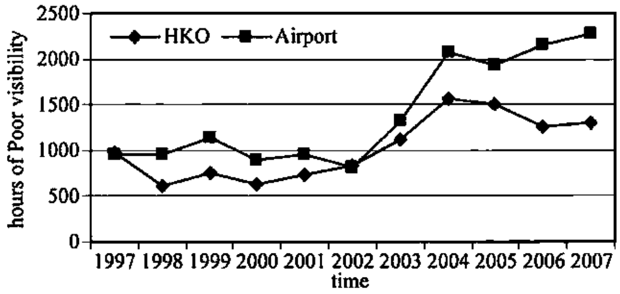


**Figure 5.** Hours of poor visibility in HKO and Airport (Data: HKO)

The scavenging of aerosols by precipitation is investigated as follows. Rain events are identified from the daily rainfall obtained form HKO. The daily API before and after the rain events are collected, and the percent changes in API computed. Figure 6 shows the changes in API as a function of rain rate for the summer and winter. Linear regression analyses are performed for the winter and summer. The slope of the regression is insignificant for the summer. In winter, the regression of the form $\delta C/C = -\alpha RR - \beta$ where $\delta C/C$ is the fractional change of API, and RR is the rain rate in mm/day and $\alpha$, $\beta$ equal 0.6 and 0.43, respectively. While $\alpha$ is significantly different from zero, $\beta$ is not. This linear relation points to the removal of aerosol by rain, particularly in winter.

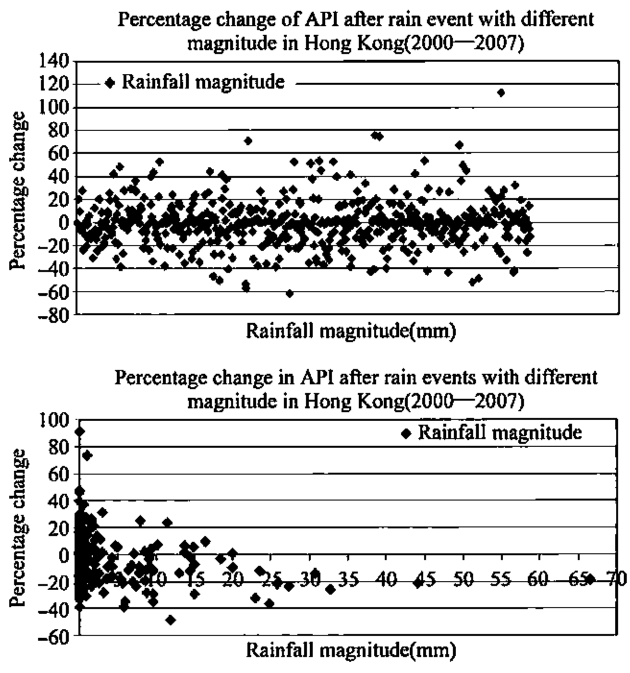


**Figure 6.** Percentage change in API after rain event as a function of daily rainfall intensity for summer (upper panel) and winter (lower panel)

## IV. DISCUSSIONS AND FUTURE WORK

This study uses a simple pollution index (API) to examine aerosol distribution in HK. This approach neglects the chemical interactions between aerosol types, water vapor, and other meteorological factors such as temperature and humidity. The aerosol concentration on eastern side of Hong Kong is lower than the western one. This phenomenon may be related to the emission locally and cross border pollutant transport from Guangzhou and Pearl River Delta (PRD). The local power plant in HK is located in Tuen Mun, which is in the western part of the New Territories. A shipping terminal port is situated in Kwai Chung. Factories are re-located to the Pearl River Delta from Hong Kong since 1980s, therefore, local emission is reduced since then and pollutions bought by factories emission shifted northward and westward to Guangzhou and Pearl River Delta. This east-west asymmetry is also noted in the AOD distribution estimated from the NASA/MODIS sensor, indicating the AOD may provide information about the large scale pollution distribution. Higher local API values for northerly wind in the winter and westerly for both seasons are also consistent with the hypothesis of cross-border transport.

API statistics are compiled separately according to the wind directions and API is a maximum for northerly wind and minimum for southerly. Assuming that the API for southerly flow is representative of the pollution condition undisturbed by cross border transport, i.e., southerly transport is zero, we estimated the impact of cross boundary transport in the summer to be approximately 33%. This is obtained by computing the average API contribution from north, east and west and dividing by the API for southerly wind. Similarly, the cross border contribution for winter is approximate 23%. With eight years of data, our analysis is not inconsistent with Lau et al.'s (2006) analysis that more than 50% (67% for summer and 77% for winter in our case) of the pollution is generated locally.

There is a clear increasing trend in aerosol concentration from 2000–2004, however, aerosol concentration started to level-off or decrease since 2004. The early increase may be explained by the worsening of cross border pollution, increases in vehicular transportation and construction works etc. The break after 2004 may be related to the passing of a series of legislations to combat pollution emission in HK (HKEDP). It should be emphasized that the effect of the new legislation generally takes 2–3 years to take effect, especially for legislations related to changing old vehicles. These policies may play an important role in contributing to the leveling off of API in Hong Kong after 2004.

The effect of aerosol on the visibility is clearly reflected in Figure 5. The time of poor visibility in the Airport is consistently higher than that at HKO, which may again reflect the west-east asymmetry. Both HKO and airport indicate (relative) maxima in 2004. While the visibility in HKO improves after 2004, the visibility continues to worsen after a decrease in 2005. Whether this is indicative of deterioration in the PRD (transport from the west affecting the Airport) and stabilization in HK (as indicated by the HKO observation) has yet to be confirmed.

The rate of wet deposition is proportional to the rain intensity, the aerosol concentration, and inversely to the cloud water content under the cloud column (Walcek, 2003). Using daily rain rate and API data, we show a linear relation between the fractional decrease of API and rainfall rate in winter. However, this relationship is not significant in summer. This may be due to the relatively low API in summer, reducing the accuracy of the fractional change. The rain intensity is also higher in summer. As discussed in Section 1, most of the pollution may be scavenged within the first hour. Aerosols may continue to be produced after the rain events. Hence it is important to use higher resolution API and rain data, such as hourly, to quantify the wet deposition effect.

## ACKNOWLEDGMENTS

This paper is an extension of an M.Sc thesis in Earth System Science submitted by KCL to the Institute of Space and Earth Information Science at CUHK. The MODIS AOD data are available from the NASA GSFC DAAC. Figure 4 in this paper is generated using GIOVANNI, an on-line software developed by the NASA/GSFC Data and Information Science Center (DISC). The meteorological and air quality data are provided by the HK Observatory and HK Environmental Protection Department. LSC acknowledges support from a Direct Grant provided by the CUHK.

## REFERENCES

[1] AMS, 2008, Glossary of meteorology, Online resources, Available at:http://amsglossary.allenpress.com/glossary/search?id=aerosol-optical-depth1, Date of Access: 31st May, 2008

[2] Baut-Menard P., Duce, R.A., 1986, Precipitation scavenging of aerosol particles over remote marine regions, Nature, 321: 508–510.

[3] Chate D. M., Rao P. S. P, Naik M. S., Momin G. A. Safai P. D., Ali K., 2003, Scavenging of aerosols and their chemical species by rain, Atmospheric Environment, 37(18): 2477–2484.

[4] Chate M. D., Pranesha T. S., 2004, Field studies of scavenging of aerosols by rain events, Journal of Aerosol Science, 35(6): 695–706.

[5] Dickinson R. E., 1996, Climate engineering a review of aerosol approaches to changing the global energy balance, Climatic Change, 33(3): 279–290.

[6] Garcia Neto, P. J., Garcia, B. A., Fernadez Diaz, J. M., Rodriguez Brana, M. A., 1994, Parametric study of selective removal of atmospheric aerosol by below-cloud scavenging. Atmospheric Environment 28, 2335–2342.

[7] He, Q., Li, C., Mao, J., Lau, A K-H, Chu DA, 2008, Analysis of aerosol vertical distribution and variability in Hong Kong, J.

Geophys. Res., 113, D14211, doi:10.1029/2008JD009778

[8] Hong Kong Environmental Protection Department (HKEPD), 2002, Study of air quality in the pearl river delta region, HKEPD HKSARG: 25–30.

[9] HKEPD, 2008, Environmental Protection Department Online Web-site, Online resources, Available at: http://www.epd.gov.hk/epd/eindex.html, Date of Access: 15th June, 2008

[10] Hong Kong Observatory, 2008, Hong Kong Observatory Online Web-site, HKSARG Online resources, Available at: http://www.hko.gov.hk

[11] Khain, A, Rosenfeld, D., Pokrovsky, A, 2005, Aerosol impact on the dynamics and microphysics of convective clouds, Q. J. R. Meteorol. Soc.,131 (611): 2639–2663.

[12] Guangzhou Environmental Protection Department, 2005, 2006, Guangzhou province environmental quality report, Guangzhou Environmental Protection Department, Online resources, Available at:http://210.72.1.33/zwgk/hjgb/, Date of Access: 12th June, 2008

[13] Oliver J. E., 2005, Encyclopedia of world climatology, Encyclopedia of World Climatology, Online resources, Available at: http://www.springerlink.com/content/u849668067237327/fulltext.html

[14] Kerker M., Hampl V., 1974, Scavenging of aerosol particles by falling water drop and calculation of washout coefficients, J. Atmo. Sci., 31(5): 1368–1376.

[15] Lawrence F., Radke L. F., Hobbs P. V., Eltgroth M.W., 1980, Scavenging of aerosol particles by precipitation, J. Appl. Meteor., 19 (6): 715–722.

[16] Lau, A. K-W, Lo, A. C. O., Gray J., Yuan Z., C. Loh, 2007, Relative significance of local vs. regional Sources: Hong Kong's air pollution, Civic Exchange, pp.36 (available from URL: www.civic-exchange.org)

[17] Lohmann U., Feichter J., 2005, Global indirect aerosol effects: a review, Atmospheric Chemistry and Physics, 5: 715–737.

[18] Lohmann U., 2006, Aerosol effects on clouds and climate, Space Sci. Rev, 125(1–4): 129–137.

[19] NASA, 2008, MODIS Terra and Aqua collection 5 analysis and intercomparison, Online resources, Available at: http://acdisc.sci.gsfc.nasa.gov/Giovanni/modis/Col005.monthly. 2.shtml#description, Date of Access: 17th May, 2008

[20] Rosenfeld, D., 1999, TRMM observed first direct evidence of smoke from forest fires inhibiting rainfall, Geophys, 26: 3105–3108.

[21] Rosenfeld, D., Woodley, W. L., 2000, Deep convective clouds with sustained supercooled liquid water down to –37.5°C, Nature, 405: 440–442.

[22] Sinkevich A. A., Dovgalyuk Yu. A., Ishenko M. A. Ponomarew Yu. F., Stepanenko V. D., Veremei N. E., 2000, Investigations of aerosol scavenging efficiency by precipitation, AIP Conf. Proc. 534 (1): 1–6.

[23] Wallace, J. M., Hobb, P. V., 1977, Atmospheric Science, An introductory survey, Academic Press, pp. 467.

[24] Yuet L. L., Sequeria R., 2002, Water-soluble aerosol and visibility degradation in Hong Kong during autumn and early winter, Environmental Pollution, 116(2): 225–233.

[25] Zhang L., Michelangeli D. V., Taylor P. A., 2005, Influence of aerosol concentration on precipitation formation in low-level, warm stratiform clouds, Journal of Aerosol Science, 37(2): 203–217.